

INFLUENCE OF GIBBSITE SURFACE AREA AND CITRATE ON Ni SORPTION MECHANISMS AT pH 7.5

NORIKO U. YAMAGUCHI^{1,*}, ANDREAS C. SCHEINOST² AND DONALD L. SPARKS³

¹ Department of Quantum Engineering and Systems Science, Graduate School of Engineering, The University of Tokyo, 7-3-1 Hongo Bunkyo-ku Tokyo, 113-8656, Japan

² Institute of Terrestrial Ecology, ETHZ, 8952 Schlieren, Switzerland

³ Department of Plant and Soil Sciences, University of Delaware, Newark, DE 19717-1303, USA

Abstract—We investigated the sorption of Ni to gibbsite of two different surface areas at pH 7.5, in the presence and absence of citrate, over a time period of 180 days. Extended X-ray absorption fine-structure spectroscopy was employed to elucidate the sorption mechanisms at the molecular level. In agreement with former results, Ni-Al layered double hydroxide (LDH) formed in the presence of gibbsite of low surface area. However, gibbsite of high surface area suppressed the formation of the surface precipitate. Instead, two Al atoms neighboring Ni at distances of 2.95–2.98 Å indicated formation of an inner-sphere sorption complex, where each NiO₆-octahedron shares edges with two AlO₆-octahedra. Focused multiple scattering arising from Al atoms at a distance of 6 Å suggest that sorbed Ni(OH)₂(OH)₂ monomers epitaxially extend the hexagonal arrangement of Al atoms in gibbsite. Only after 30 days or more was a small amount of LDH formed. The presence of citrate prevented the formation of LDH, while maintaining the formation of inner-sphere sorption complexes.

Key Words—Citrate, EXAFS, Gibbsite, Layered Double Hydroxide, Ni, Sorption, Surface Area, Surface Precipitate.

INTRODUCTION

The pollution of soils and sediments by heavy metals has deleterious effects on the health of ecosystems. Naturally-occurring processes that sequester metals to immobile solids within aqueous systems can minimize these effects. A comprehensive understanding of the mechanisms and rates of the sorption processes that stabilize hazardous metals is necessary to predict the metal stabilization capacity of soil or sediment and the future risk. Phyllosilicates, metal (hydr)oxides, and humic substances adsorb heavy metals by formation of inner- or outer-sphere sorption complexes, creating important sinks for these metals in ecosystems (Sparks *et al.*, 1999). The long-term contact of heavy metals with soil materials may further reduce their extractability and mobility (McLaren *et al.*, 1998). This phenomenon, called an ‘ageing effect’, can be explained by a variety of processes, including surface diffusion into porous minerals (Brummer *et al.*, 1988; Scheinost *et al.*, 2001), formation of surface-induced precipitates (O’Day *et al.*, 1994; Scheidegger *et al.*, 1997) and the subsequent modification of these precipitates in terms of crystal structure, crystal composition and particle size (Ford *et al.*, 1999; Charlet and Manceau, 1994; Schlegel *et al.*, 1999).

Several studies at circum-neutral pH indicate the role of the mineral surface in determining the end-product of the retention process (Ford *et al.*, 2001). Weathering of the sorbent surface leads to the release of elements

which may then re-precipitate with the sorbate to form a new mineral. Examples for this are the release of Al from Al-containing phyllosilicates and gibbsite to form metal-containing LDH (Scheidegger *et al.*, 1997), and the release of Si from phyllosilicates or quartz to form new metal-containing phyllosilicate-like phases by precipitation from solution (Charlet and Manceau, 1994; Manceau *et al.*, 1999) or by transformation from an intermediate LDH phase (Ford *et al.*, 1999). However, even without the dissolution of the sorbent phase, surface precipitation may be induced by increasing the concentration of ions in the electrical double layer and by providing a structural template, both processes lowering the barrier of nucleation. An example is the epitaxial growth of a Co-containing Ti oxide phase at the surface of the relatively stable, Ti oxide mineral rutile (O’Day *et al.*, 1996).

A third process directing the sorbate sequestration is the surface loading. While at lower loadings inner-sphere sorption complexes prevail, precipitates may form at higher loadings (O’Day *et al.*, 1996). It is evident that the surface loading at given amounts of metals and solids is determined by the number of available surface sites. This suggests that the surface area may also be a key factor controlling the sorption product.

Previous studies using gibbsite of relatively low surface area of 25 m²/g found that α -Ni hydroxide was formed first, followed by Ni-Al LDH formation at pH 7.5 (Scheidegger *et al.*, 1997; Scheinost *et al.*, 1999; Scheinost and Sparks, 2000; Yamaguchi *et al.*, 2001). When citrate was added, total Ni retention was reduced

* E-mail address of corresponding author: n-yamaguchi@q.t.u-tokyo.ac.jp

and an α -Ni hydroxide phase became dominant instead of LDH. The rate-limiting step for the formation of Ni-Al LDH on Al-bearing minerals was Al dissolution from the mineral surface (Scheidegger *et al.*, 1998). In the presence of citrate, however, Al formed an aqueous complex with citrate, thus preventing its coprecipitation with Ni hydroxide to form LDH (Yamaguchi *et al.*, 2001).

The objective of the present study was to investigate the influence of surface area on Ni sequestration in the ternary Ni-gibbsite-citrate system over time. In addition to the gibbsite of lower surface area, which was already employed in a former study, we used a gibbsite with significantly higher surface area to increase the number of active surface sites. This should allow us to investigate whether there is competition between precipitate formation and formation of inner-sphere sorption complexes. Citrate which complexes with both Ni and Al was selected as an additional variable, representing natural organic ligands exuded by some plant species to acquire mineral nutrients from soil (Jones, 1998).

MATERIALS AND METHODS

Sorbents

Gibbsite with high surface area (HS-Gb, $96 \text{ m}^2 \text{ g}^{-1}$) was precipitated from $1 \text{ mol L}^{-1} \text{ AlCl}_3$ at pH 4.6, followed by a 36 day dialysis in deionized water (Kyle *et al.*, 1975). X-ray diffraction patterns and Fourier transform infrared (FTIR) spectra showed that HS-Gb was pure gibbsite, free from detectable impurities. The gibbsite with low surface area (LS-Gb, $25 \text{ m}^2 \text{ g}^{-1}$) is from a natural clay deposit (Arkansas, USA; Wards) and contains ~10% bayerite. The point of zero salt effect (PZSE) as determined by batch titration at ionic strengths of 0.01, 0.1 and 1 M (Schulthess and Sparks, 1986) was 10.1 for HS-Gb and 9.0 for LS-Gb.

Sorption of Ni and citrate

HS-Gb and LS-Gb samples were hydrated in $1.5 \text{ mmol L}^{-1} \text{ NaClO}_4$ solution for 24 h, then the pH was pre-adjusted to 7.5 using 0.1 mol L^{-1} of NaOH and kept constant for 2 h. The solid/solution ratio was adjusted to 20 g L^{-1} with $1.5 \text{ mmol L}^{-1} \text{ NaClO}_4$. To this suspension we slowly added 0.1 mol L^{-1} of $\text{Ni}(\text{ClO}_4)_2$ solution, 0.1 mol L^{-1} of sodium citrate solution, or mixtures of both which had been equilibrated for 2 h, in order to achieve initial concentrations of [Ni] and/or [citrate] of 1.5 mmol L^{-1} . The pH of the sodium citrate and $\text{Ni}(\text{ClO}_4)_2$ -citrate solutions was adjusted to pH 7.5 before adding to the gibbsite suspension, whereas the pH of the $\text{Ni}(\text{ClO}_4)_2$ solution was not adjusted to avoid supersaturation with respect to $\text{Ni}(\text{OH})_2$. During the first 24 h of sorption, pH was maintained at 7.50 by automatic addition of 0.1 mol L^{-1} NaOH or HClO_4 using a pH-stat system (Radiometer, Copenhagen). The suspension was stirred with a Teflon stir bar and purged

with N_2 gas to prevent CO_2 contamination. After 24 h, the suspensions were shaken on an orbital shaker and the pH of the suspension was adjusted manually if necessary. Ten mL of suspension were sampled periodically (20 min–90 days) and centrifuged at 26950 g for 3 min. The supernatant liquid was filtered through a $0.2 \mu\text{m}$ membrane filter and analyzed for Ni and Al by inductively coupled plasma atomic emission spectroscopy (ICP-AES). Total citrate concentration in solution was determined by high-performance liquid chromatography (HPLC) (Thermo Separation Products Spectra System, AS3000, Alltech IOA-2000 column) after removing Na and Ni with a cation exchange resin (Maxi Clean IC-H, Alltech) at $\text{pH} < 2$. The sorbed amounts of Ni and citrate were calculated from the difference between initial and final concentrations in solution.

For extended X-ray absorption fine structure (EXAFS) analysis, selected samples were washed twice with $0.1 \text{ mol L}^{-1} \text{ NaClO}_4$ adjusted to pH 7.5, then centrifuged at 26950 g for 3 min. The wet pastes were sealed with parafilm and stored in a refrigerator for subsequent EXAFS analysis.

EXAFS spectroscopy

X-ray absorption spectra were collected at beamline X-11 A at the National Synchrotron Light Source, Brookhaven National Laboratory, Upton, New York. The electron storage ring operated at 2.8 GeV with a beam current varying between 120 and 330 mA. The beam height was adjusted by a vertical slit width of 0.5 mm before entering the Si(111) crystal monochromator. Higher-order harmonics were suppressed by detuning the monochromator by 25%. The monochromator position was calibrated by assigning the first inflection the K-absorption edge of metallic Ni foil to 8333.0 eV . Fluorescence spectra were collected using an Ar-filled Stern-Heald detector with Soller slits and a Co-3 filter (Lytle *et al.*, 1984). The incoming beam was measured with an N_2 -filled ion chamber. Wet pastes of Ni-reacted minerals were mounted in Al holders and covered with Mylar foil. At least three scans were collected at room temperature, using the following parameters (photon energies relative to E_0): -200 to -30 eV in 10 eV steps and 1 s counting time per step; -30 to 30 eV in 0.5 eV steps at 1 s per step; 30 eV to 14.5 \AA^{-1} in 0.07 \AA^{-1} steps at 5 s.

All steps of the EXAFS data reduction were performed using the WinXAS 97 1.1 software package (Ressler, 1997). The spectra were normalized by fitting second-degree polynomials to the pre-edge and post-edge regions. The position of the pre-edge peak of Ni^{2+} was used to check for energy shifts between single scans before averaging. The energy axis (eV) was converted to photoelectron wave vector units (\AA^{-1}) by assigning the origin, E_0 , to the first inflection point of the absorption edge. The EXAFS backscattering signal was isolated

from the absorption edge background by using a cubic spline function with six segments. The resulting $\chi(k)$ functions were weighed by k^3 to account for the damping of oscillations with increasing k , and Fourier-transformed to achieve radial structure functions (RSF). A Bessel window with a smoothing parameter of 4 was used to suppress artifacts due to the finite Fourier filtering range of 1.5 and 12.5 \AA^{-1} .

Theoretical scattering paths were calculated with FEFF 7.02 (Rehr *et al.*, 1991). The structure of lizardite was used to simulate the paths of Ni-Al LDH and α -Ni hydroxide by substituting Ni and Al for Mg, and omitting the tetrahedral silicate sheet. The structure of gibbsite (Saalfeld and Wedde 1974), with Al partly replaced by Ni, was used to model inner-sphere surface complexes. Multishell fits were performed in R space using an amplitude reduction factor, S_0^2 , of 0.85 (O'Day *et al.*, 1994).

RESULTS AND DISCUSSION

Influence of surface area

Table 1 gives Ni sorption data as a function of surface area, citrate and time. Without citrate, HS-Gb removed 95 wt.% of Ni from solution within one day, while LS-Gb removed only 23 wt.%. However, this value increased to 53 wt.% during the following 30 days. Although LS-Gb sorbed less Ni on a weight basis, surface loadings per unit surface area were about twice as high as for HS-Gb.

Table 1. Ni sorption by LS-Gb and HS-Gb at pH 7.5 in the presence and absence of citrate.

	Reaction time	Ni sorbed (mmol/kg)	Ni sorbed (mmol/m ²)	Ni removed (%)
LS-Gb Ni only	24 h	17	0.68	23
	3 d	28	1.1	38
	30 d	39	1.6	53
HS-Gb Ni only	24 h	68	0.71	95
	30 d	71	0.74	98
	90 d	71	0.74	98
	180 d	71	0.74	98
LS-Gb Ni-citrate	24 h	7.0	0.28	10
	3 d	8.2	0.32	11
	30 d	15	0.58	20
HS-Gb Ni-citrate	24 h	54	0.56	74
	30 d	59	0.62	82
	90 d	70	0.73	97
	180 d	72	0.75	99

Figure 1 shows the EXAFS χ functions on the left and the corresponding Fourier transforms, which are radial structure functions (RSF), on the right. The RSF of LS-Gb shows three pronounced peaks at ~ 1.7 , 2.6 and 5.7 \AA (uncorrected for phase shift). The first peak was fit with 6 O atoms surrounding Ni at a distance of 2.05 \AA in octahedral configuration (Table 2). The second peak was fit by 4.2 Ni atoms at a distance of 3.06 \AA from the central Ni atom. The distances and coordination numbers are in accordance with a Ni-Al LDH (Scheidegger *et al.*,

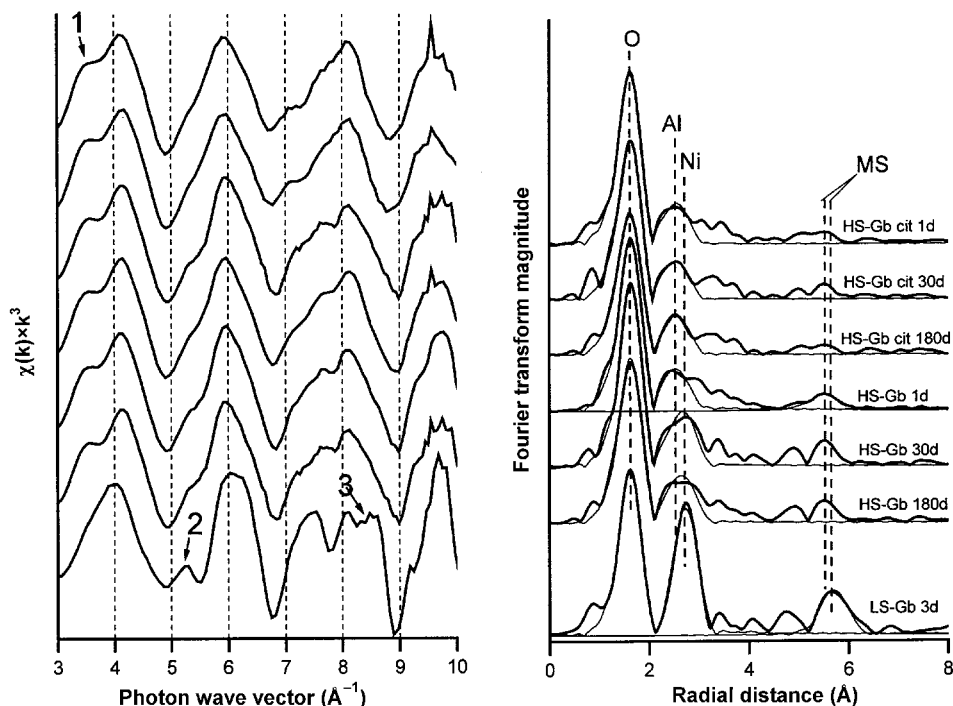


Figure 1. χ functions (left) and radial structure functions (right) of Ni-reacted gibbsite samples with high surface area (HS-Gb). For comparison, a Ni-reacted gibbsite of low surface area (LS-Gb) is shown at the bottom. See Table 2 for an explanation of the labels.

Table 2. NiK α EXAFS fit results of Ni-citrate-gibbsite ternary and Ni-gibbsite binary systems.

Gibbsite	Citrate	Reaction time	Ni-O			Ni-Al			Ni-Ni			MS		
			CN ^(*)	R ^(#)	$\sigma^{2(\dagger)}$	CN ^(*)	R ^(#)	$\sigma^{2(\dagger)}$	CN ^(*)	R ^(#)	$\sigma^{2(\dagger)}$	CN ^(*)	R ^(#)	$\sigma^{2(\dagger)}$
LS-Gb		3 d	6.5	2.05	0.004	–	–	–	3.6	3.06	0.004	6.0	6.13	0.004
HS-Gb		1 d	6.1	2.05	0.003	1.6	2.95	0.001	–	–	–	5.4	6.03	0.010
HS-Gb		30 d	6.0	2.05	0.003	1.1	2.95	0.003	1.0	3.06	0.003	–	–	–
HS-Gb		180 d	6.8	2.05	0.005	1.4	2.95	0.004	1.0	3.06	0.004	–	–	–
HS-Gb	+	1 d	6.0	2.05	0.004	1.8	2.98	0.002	–	–	–	–	–	–
HS-Gb	+	30 d	6.0	2.05	0.004	2.1	2.98	0.003	–	–	–	6.4	6.01	0.008
HS-Gb	+	180 d	6.4	2.05	0.006	1.7	2.98	0.001	–	–	–	6	6.02	0.015

* Coordination number, estimated confidence interval ± 0.75

Radial distance (\AA), estimated confidence interval $\pm 0.01 \text{\AA}$

† Debye-Waller factor (\AA^2), estimated confidence interval $\pm 0.001 \text{\AA}^2$

1998). Because the electron waves backscattering from Ni and Al atoms at a distance of 3.06 \AA are almost exactly out of phase, Al in the second coordination sphere reduces the backscattering from Ni. Consequently, Al atoms cannot be fit reliably, and the fitted coordination numbers of Ni are smaller than expected (Scheinost and Sparks, 2000). Furthermore, the beats at 5.3 \AA^{-1} and 8 \AA^{-1} in the χ function (arrows 2 and 3 in Figure 1) are due to focused multiple scattering paths involving both Ni and Al at a distance of $\sim 6.12 \text{\AA}$. These beats allow us to discriminate Ni-Al LDH from other, similar phases such as defect Ni hydroxide layers or phyllosilicates (Scheinost and Sparks, 2000). In fact, the peak at $\sim 5.7 \text{\AA}$ in the RSF could be fit with a Ni-Al-Ni triple scattering path with a distance of 6.13 \AA (Table 2). Thus, the EXAFS data show that a Ni-Al LDH phase has formed after reacting LS-Gb with Ni. These results have been further confirmed by using diffuse reflectance spectroscopy (DRS) (Scheinost *et al.*, 1999; Yamaguchi *et al.*, 2001).

In contrast, the RSF of the HS-Gb samples generally lack the strong Ni backscattering of precipitate compounds (Figure 1). While the fit results of the first shell indicate the same octahedral coordination of Ni to oxygen, the relatively weak second-shell peaks could be fit with ~ 2 Al atoms at a distance of 2.95–2.98 \AA (Table 2). This distance is intermediate to that of the Ni–Ni, Al distance in Ni-Al LDH (3.06 \AA) and to the Al–Al distance in gibbsite (2.93 \AA) (Saalfeld and Wedde, 1974). This distance and the coordination number of 2 are in accordance with an inner-sphere sorption complex, where Ni octahedra share edges with two adjacent Al octahedra.

In spite of the weak second-shell backscattering, the RSF of the HS-Gb samples show pronounced backscattering out to 6 \AA (Figure 1). As Fourier-backtransforms of selected RSF regions showed, the RSF peaks between 5 and 6 \AA are responsible for the beat at 3.5 \AA^{-1} in the χ spectra (arrow 1 in Figure 1). For one sample (HS-Gb 24h), the RSF peak at $\sim 5.2 \text{\AA}$ could be fit by a Ni-Al-Al multiple scattering path 6.03 \AA long (Table 2). This distance is about twice the distance of the single Ni-Al paths, therefore indicating a focused

multiple scattering phenomenon similar to that in Ni-Al LDH (Scheinost and Sparks, 2000). A similar beat pattern has been observed for transition metals incorporated in the Al hydroxide sheets of lithiophorite or chlorite (Manceau *et al.*, 1987, 2000; Scheinost *et al.*, 2002). Therefore, the χ beat pattern observed for all HS-Gb samples, and the RSF peaks at $\sim 5.2 \text{\AA}$ observed for samples HS-Gb cit 24h, HS-Gb cit 30d, and HS-Gb 24h indicate that Ni substitutes for Al, occupying the same crystallographic position in the hexagonal gibbsite sheets. However, only positions near the surface are occupied, as is indicated by the second-shell coordination number of two (Table 2). Thus, the gibbsite structure acts as a template for the formation of inner-sphere Ni sorption complexes, as is depicted in Figure 2. No further epitaxial growth of Ni hydroxide seems to occur, hence the Ni hydroxide monomers terminate the gibbsite sheets. The most likely explanation is the size incompatibility between Ni hydroxide (Ni–Ni distances in hydroxides $> 3.06 \text{\AA}$; Scheinost and Sparks, 2000) and Al hydroxide (Al–Al distances in gibbsite: 2.93 \AA ; Saalfeld and Wedde, 1974).

While all spectra for HS-Gb showed the characteristic beat pattern at 3.5 \AA^{-1} and could be fit with an Al shell at $\sim 2.95 \text{\AA}$, the spectra of the citrate-free samples collected after 30 and 180 days required the fit of an additional Ni shell at 3.06 \AA . The coordination numbers of one could indicate the sorption of Ni hydroxide

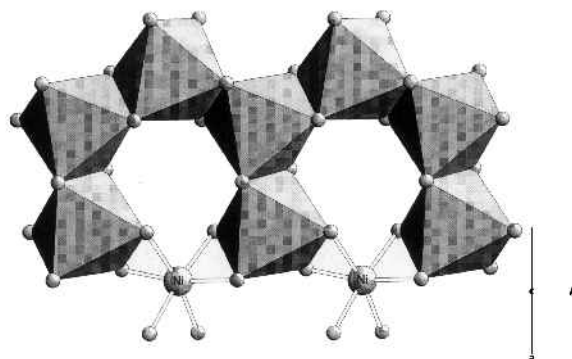


Figure 2. Model for the inner-sphere sorption of Ni at the gibbsite surface.

dimers. However, the structure of the MS (multiple scattering) peaks approaches that of LS-Gb, indicating formation of LDH. Since the main features indicative of inner-sphere sorption complexes remained, however, only a small amount of LDH may have formed in these samples.

Previous results have suggested that the presence of Al hydroxide of relatively high solubility is a requirement for the rapid formation of LDH (Taylor, 1984). Consequently, the faster formation of Ni-Al LDH in the presence of pyrophyllite as compared to gibbsite has been explained by secondary precipitation of amorphous Al hydroxide that was induced by pyrophyllite dissolution at pH 7.5 (Yamaguchi *et al.*, 2001). Since minerals with higher surface area tend to dissolve faster (Sutheimer *et al.*, (1999), we would have expected that the presence of gibbsite with high surface area accelerates the formation of LDH. However, we observed that the formation of the inner-sphere sorption complex outcompeted the formation of LDH. If we assume that both LS-Gb and HS-Gb have the same surface sites, the energy required for the formation of the surface complex should also be the same. Hence, the higher Ni surface loading on LS-Gb, and consequently the higher saturation index with respect to the formation of LDH, may be the main reason why LDH formed only at the surface of LS-Gb.

Influence of citrate

Citrate generally reduced Ni sorption, but the effect was more pronounced for LS-Gb than for HS-Gb (Table 1). For instance, citrate had reduced the Ni sorption of HS-Gb by 30%, but that of LS-Gb by 60% after 1 day of reaction. The EXAFS spectra in Figure 2 and the fit data in Table 2 clearly show that the Ni sorption mechanism on HS-Gb was not influenced by citrate, *i.e.* the same inner-sphere sorption complex formed. In contrast, previous DRS results have shown

that citrate inhibited the formation of LDH in the presence of LS-Gb and an α -Ni hydroxide precipitate was formed instead (Yamaguchi *et al.*, 2001).

Macroscopic investigations of metal-ligand systems revealed that complexing ligands both enhance and suppress metal sorption depending on pH (Kraemer *et al.*, 1998). The structure of a ternary complex was spectroscopically confirmed by electron paramagnetic resonance (EPR) (McBride, 1985), and EXAFS (Alcacio *et al.*, 2001; Bargar *et al.*, 1998; Bargar *et al.*, 1999; Fitts *et al.*, 1999; Ostergren *et al.*, 2000a,b). The existence of complexing ligands which forms very stable complexes with metals can drastically alter the metal structure on mineral surfaces. In the binary metal-sorbent system and in the presence of chloride, sulfate, and carbonate, Pb sorbed on the goethite surface as an inner-sphere complex (Bargar *et al.*, 1998; Ostergren *et al.*, 2000a,b) whereas in the presence of EDTA, sorbed Pb forms an outer-sphere complex (Bargar *et al.*, 1999).

There were no further indications of a structural change of the surface complexes induced by citrate. In principle, ternary Ni-citrate-surface complexes may form in two ways. First, citrate may form a bridge between Ni and gibbsite (type A ternary complex). In this case, Ni atoms would be surrounded by O and C atoms only within the first 3.5 Å. Having 2 Al atoms at a distance of 2.98 Å clearly eliminates this type of complex. Second, Ni may form a bridge between gibbsite and citrate (type B ternary complex). In this case, 2 Al atoms would be observable as for a binary Ni-gibbsite surface complex. Due to the weak backscattering and similarity to O, the second shell C atom of the citrate-Ni bond would not be visible. The only noticeable difference from a binary complex could be a slight increase of interatomic distances which has been explained by the replacement of water with a ligand of weaker ligand field strength (Burns, 1993). Alcacio *et al.* (2001) observed such an increase in Cu-O distances

Table 3. Citrate sorption by LS-Gb and HS-Gb at pH 7.5 in the equimolar presence and absence of Ni.

	Reaction time	Citrate sorbed (mmol/kg)	Citrate sorbed (mmol/m ²)	Citrate removed (%)
HS-Gb citrate only	24 h	59	0.60	74
	30 d	63	0.64	79
	90 d	63	0.64	79
HS-Gb Ni-citrate	24 h	61	0.62	76
	30 d	72	0.73	90
	90 d	74	0.76	92
	180 d	79	0.81	99
LS-Gb citrate only	24 h	7.1	0.28	9.2
	3 d	9.7	0.39	13
	30 d	44	1.8	58
LS-Gb Ni-citrate	24 h	4.5	0.18	4.2
	30 d	3.3	0.13	7.1
	90 d	5.2	0.21	6.5

after formation of Cu-humate, type B ternary complexes. However, our data do not show a change in the Ni–O distance in the presence of citrate (Table 2). In the structure of $[\text{Ni}(\text{Hcit})(\text{H}_2\text{O})_2]^{2-}$, Ni–O bond distances vary from 2.020 to 2.074 Å depending on the ligand type associated with Ni (Zhou *et al.*, 1997). Therefore, no evidence for the formation of type B ternary complexes is given by EXAFS. However, macroscopic data might suggest the existence of type B ternary complexes. Citrate uptake by HS-Gb increased in the presence of Ni. Corresponding to the increase of Ni sorption with time, citrate uptake also increased (Table 3). These results indicate that sorbed Ni provided sorption sites for citrate. According to speciation calculations (MINEQL version 4.1) the Ni-citrate 1:1 complex is the dominant species at pH 7.50. It is therefore possible that sorbed citrate is associated with Ni on HS-Gb as a type B ternary complex. However, FTIR spectra of citrate sorbed to HS-Gb did not vary in the presence and absence of Ni. Further investigations are required to provide evidence for the existence of the type B ternary complex.

CONCLUSIONS

The Ni sorption mechanism at pH 7.5 was influenced by gibbsite surface area. At low surface area and corresponding high surface loading, a Ni-Al LDH precipitate formed. At high surface area and lower surface loading, formation of an inner-sphere surface complex prevailed. The inner-sphere sorption complexes were formed by using the structure of gibbsite as a template. Rather than extending the gibbsite structure epitaxially, however, the surface complex monomers terminated the gibbsite surface. A small amount of Ni-Al LDH formed only after an extended ageing period. Citrate generally reduced the amount of Ni sorbed, but the effect was more pronounced for LS-Gb than for HS-Gb. Furthermore, citrate prevented the formation of an accessory LDH phase.

ACKNOWLEDGMENTS

This research was supported by the Japan Securities Scholarship Foundation and a JSPS research fellowship for young scientists. We would like to express our gratitude to Dr M. Radosevich, University of Delaware, for his generous assistance with the use of the HPLC. The critical reviews by Drs M.B. McBride and W.F. Bleam are acknowledged.

REFERENCES

- Alcacio, T.E., Hesterberg, D., Chou, J.W., Martin, J.D., Beauchemin, S. and Sayers, D.E. (2001) Molecular scale characteristics of Cu(II) bonding in goethite-humate complexes. *Geochimica et Cosmochimica Acta*, **65**, 1355–1366.
- Bargar, J.R., Brown, G.E., Jr. and Parks, G.A. (1998) Surface complexation of Pb(II) at oxide-water interfaces: III. XAFS determination of Pb(II) and Pb(II)-chloro adsorption complexes on goethite and alumina. *Geochimica et Cosmochimica Acta*, **62**, 193–207.
- Bargar, J.R., Persson, P. and Brown, G.E., Jr. (1999) Outer-sphere adsorption of Pb(II)EDTA on goethite. *Geochimica et Cosmochimica Acta*, **63**, 2957–2969.
- Bruemmer, G.W., Gerth, J. and Tiller, K.G. (1988) Reaction kinetics of the adsorption and desorption of nickel, zinc and cadmium by goethite. I. Adsorption and diffusion of metals. *Journal of Soil Science*, **39**, 37–52.
- Burns, R.G. (1993) *Mineralogical Applications of Crystal Field Theory*. Cambridge University Press, New York.
- Charlet, L. and Manceau, A. (1994) Evidence for the neoformation of clays upon sorption of Co(II) and Ni(II) on silicates. *Geochimica et Cosmochimica Acta*, **58**, 2577–2582.
- Fitts, J.P., Persson, P., Brown, G.E., Jr. and Parks, G.A. (1999) Structure and bonding of Cu(II)-glutamate complexes at the gamma-Al₂O₃-water interface. *Journal of Colloid and Interface Science*, **220**, 133–147.
- Ford, R.G., Scheinost, A.C., Scheckel, K.G. and Sparks, D.L. (1999) The link between clay mineral weathering and the stabilization of Ni surface precipitates. *Environmental Science and Technology*, **33**, 3140–3144.
- Ford, R.G., Scheinost, A.C. and Sparks, D.L. (2001) Frontiers in Metal Sorption/Precipitation Mechanisms on Soil Mineral Surfaces Pp. 41–62 in: *Advances in Agronomy*, **74**, (D.L. Sparks, editor). American Society of Agronomy, Madison, Wisconsin.
- Jones, D.L. (1998) Organic acids in the rhizosphere – a critical review. *Plant and Soil*, **205**, 25–44.
- Kraemer, S.M., Chiu, V.Q. and Hering, J.G. (1998) Influence of pH on competitive adsorption on the kinetics of ligand-promoted dissolution of aluminum oxide. *Environmental Science and Technology*, **32**, 2876–2882.
- Kyle, J.H., Posner, A.M. and Quirk, J.P. (1975) Kinetics of isotopic exchange of phosphate adsorbed on gibbsite. *Journal of Soil Science*, **26**, 32–43.
- Lytle, F.W., Greefgor, R.B., Sandstrom, D.R., Marques, E.C., Wong, J., Spiro, C.L., Huffman, G.P. and Huggins, F.E. (1984) Measurement of soft-X-ray absorption spectra with a fluorescence-chamber detector. *Nuclear Instruments and Methods in Physics Research Section A—Accelerators, Spectrometers, Detectors and Associated Equipment*, **226**, 542–548.
- Manceau, A., Llorca, S. and Calas, G. (1987) Crystal chemistry of cobalt and nickel in lithiophorite and asbolane from New Caledonia. *Geochimica et Cosmochimica Acta*, **51**, 105–113.
- Manceau, A., Schlegel, M., Nagy, K.L. and Charlet, L. (1999) Evidence for the formation of trioctahedral clay upon sorption of Co²⁺ on quartz. *Journal of Colloid and Interface Science*, **220**, 181–197.
- Manceau, A., Schlegel, M.L., Musso, M., Sole, V.A., Gauthier, C., Petit, P.E., Trolard, F. (2000) Crystal chemistry of trace elements in natural and synthetic goethite. *Geochimica et Cosmochimica Acta*, **64**, 3643–3661.
- McBride, M.B. (1985) Influence of glycine on Cu²⁺ adsorption by microcrystalline gibbsite and boehmite. *Clays and Clay Minerals*, **33**, 397–402.
- McLaren, R.G., Backes, C.A., Rate, A.W. and Swift, R.S. (1998) Cadmium and cobalt desorption kinetics from soil clays; effect of sorption period. *Soil Science Society of America Journal*, **62**, 332–337.
- O'Day, P.A., Brown, G.E., Jr. and Parks, G.A. (1994) X-ray-absorption spectroscopy of cobalt(II) multinuclear surface complexes and surface precipitates on kaolinite. *Journal of Colloid and Interface Science*, **165**, 269–289.
- O'Day, P.A., Chisholm-Brause, C.J., Towle, S.N., Parks, G.A. and Brown, G.E., Jr. (1996) X-ray absorption spectroscopy

- of Co(II) sorption complexes on quartz (α -SiO₂) and rutile (TiO₂). *Geochimica et Cosmochimica Acta*, **60**, 2515–2532.
- Ostergren, J.D., Brown, G.E., Jr., Parks, G.A. and Persson, P. (2000a) Inorganic ligand effects on Pb(II) sorption to goethite (α -FeOOH). II.—Sulfate. *Journal of Colloid and Interface Science* **225**, 483–493.
- Ostergren, J.D., Trainor, T.P., Bargar, J.R., Brown, G.E., Jr. and Parks, G.A. (2000b) Inorganic ligand effects on Pb(II) sorption to goethite (α -FeOOH) – I. Carbonate. *Journal of Colloid and Interface Science* **225**, 466–482.
- Rehr, J.J., Mustre de Leon, J., Zabinsky, S. and Albers, R.C. (1991) Theoretical X-ray absorption fine-structure standards. *Journal of the American Chemical Society*, **113**, 5135–5140.
- Ressler, T. (1997) WinXAS: A new software package not only for the analysis of energy-dispersive XAS data. *Journal de Physique IV*, **7**, (C2) 269–270.
- Saalfeld, H. and Wedde, M. (1974) Refinement of the crystal structure of gibbsite, Al(OH)₃. *Zeitschrift für Kristallographie*, **139**, 129–135.
- Scheidegger, A.M., Lamble, G.M. and Sparks, D.L. (1997) Spectroscopic evidence for the formation of mixed-cation hydroxide phases upon metal sorption on clays and aluminum oxides. *Journal of Colloid and Interface Science*, **186**, 118–128.
- Scheidegger, A.M., Strawn, D.G., Lamble, G.M. and Sparks, D.L. (1998) The kinetics of mixed Ni-Al hydroxide formation on clay and aluminum oxide minerals: A time-resolved XAFS study. *Geochimica et Cosmochimica Acta*, **62**, 2233–2245.
- Scheinost, A.C. and Sparks, D.L. (2000) Formation of layered single- and double-metal hydroxide precipitates at the mineral/water interface: A multiple-scattering XAFS analysis. *Journal of Colloid and Interface Science*, **223**, 167–178.
- Scheinost, A.C., Ford, R.G. and Sparks, D.L. (1999) The role of Al in the formation of secondary Ni precipitates on pyrophyllite, gibbsite, talc, and amorphous silica: A DRS study. *Geochimica et Cosmochimica Acta*, **63**, 3193–3203.
- Scheinost, A.C., Abend, S., Pandya, K.I. and Sparks, D.L. (2001) Kinetic controls on Cu and Pb sorption by ferrihydrite. *Environmental Science and Technology*, **35**, 1090–1096.
- Scheinost, A.C., Kretzschmar, R., Pfister, S. and Roberts, D.R. (2002) Combining selective sequential extractions, X-ray absorption spectroscopy and principal component analysis for quantitative zinc speciation in soil. *Environmental Science and Technology*, (in press).
- Schlegel, M., Manceau, A., Chateigner, D. and Charlet, L. (1999) Sorption of metal ions on clay minerals. I. Polarized EXAFS evidence for the adsorption of Co on the edges of hectrite particles. *Journal of Colloid and Interface Science*, **215**, 140–158.
- Schultness, C.P. and Sparks, D.L. (1986) Back titration technique for proton isotherm modeling of oxide surfaces. *Soil Science Society of America Journal*, **50**, 1406–1411.
- Sparks, D.L., Scheidegger, A.M., Strawn, D.G. and Scheckel, K.G. (1999) Kinetics and mechanisms of metal sorption at the mineral-water interface. Pp. 108–113 in: *Mineral-Water Interfacial Reactions. Kinetics and Mechanisms* (D.L. Sparks and T.J. Grundl, editors). ACS symposium series **715**. American Chemical Society, Washington, D.C.
- Sutheimer, S.H., Maurice, P.A. and Zhou, Q. (1999) Dissolution of well and poorly crystallized kaolinites: Al speciation and effects of surface characteristics. *American Mineralogist*, **84**, 620–628.
- Taylor, R.M. (1984) The rapid formation of crystalline double hydroxy salts and other compounds by controlled hydrolysis. *Clay Minerals*, **19**, 591–603.
- Yamaguchi, N.U., Scheinost, A.C. and Sparks, D.L. (2001) Surface-induced nickel hydroxide precipitation in the presence of citrate and salicylate. *Soil Science Society of America Journal*, **65**, 729–736.
- Zhou, Z.H., Lin, Y.J., Zhang, H.B., Lin, G.D. and Tsai, K.R. (1997) Syntheses, structures, and spectroscopic properties of nickel(II) citrate complexes, (NH₄)₂[Ni(Hcit)(H₂O)₂]₂·2H₂O and (NH₄)₄[Ni(Hcit)₂]₂·2H₂O. *Journal of Coordination Chemistry*, **42**, 131–141.

(Received 14 January 2002; revised 29 April 2002; Ms. 625; A.E. William J. Bleam)